Chem

CellPress

Article

Mapping the Surface Groups of Amine-Rich Carbon Dots Enables Covalent Catalysis in Aqueous Media

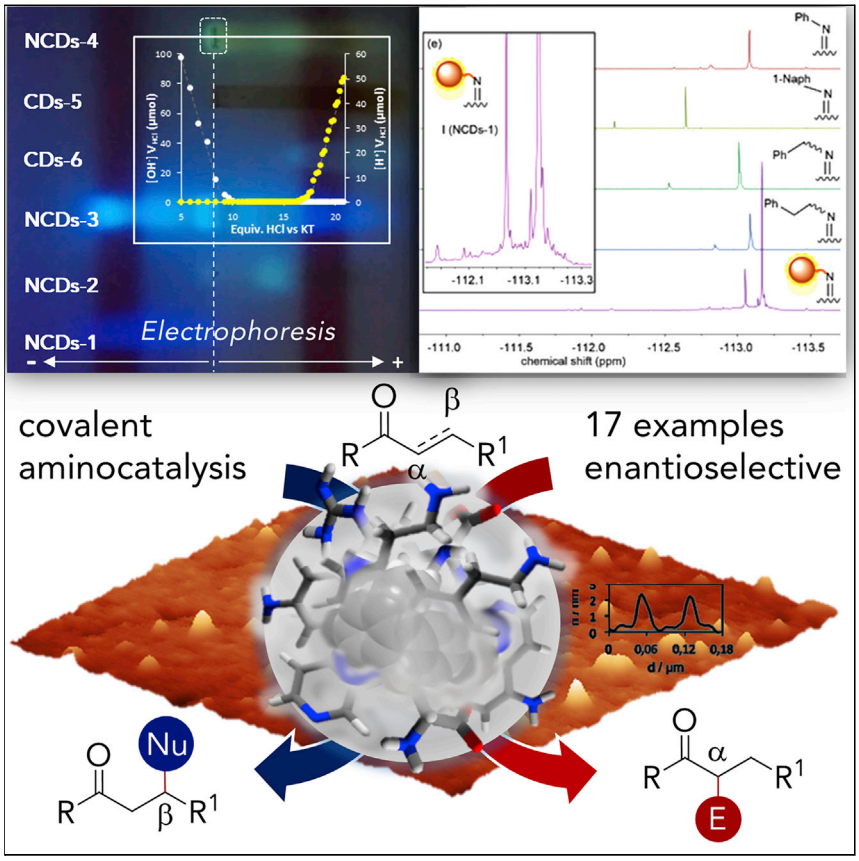

A detailed characterization of nitrogen-rich carbon dots (NCDs) has been instrumental in unlocking their potential as novel colloidal organocatalysts in water media. As a result of their multi-functional properties, diverse aminocatalytic transformations of carbonyl compounds are efficiently mediated by NCDs under iminium-ion and enamine activation pathways. These include conjugate additions and aldol reactions occurring with remarkable efficiency (up to 96% yield) and complete diastereocontrol (d.r. >20:1) and are amenable to asymmetric catalysis applications in the presence of chiral NCDs.

Giacomo Filippini, Francesco Amato, Cristian Rosso, ..., Luca Dell'Amico, Marcella Bonchio, Maurizio Prato

gfilippini@units.it (G.F.)
gragazzon@units.it (G.R.)
xavier.companyo@unipd.it (X.C.)
prato@units.it (M.P.)

HIGHLIGHTS

Multi-amino groups of NCDs are mapped at the molecular level

Reactive enamine and iminium intermediates form on the dot surface in water media

NCDs catalyze nucleophilic and electrophilic additions to carbonyl compounds

The use of chiral NCDs enables asymmetric aminocatalytic schemes

Filippini et al., Chem 6, 3022–3037
November 5, 2020
https://doi.org/10.1016/j.chempr.2020.08.009

CellPress

Chem

Article

Mapping the Surface Groups of Amine-Rich Carbon Dots Enables Covalent Catalysis in Aqueous Media

Giacomo Filippini,[1,*] Francesco Amato,[1] Cristian Rosso,[1] Giulio Ragazzon,[1,5,*] Alberto Vega-Peñaloza,[2] Xavier Companyó,[2,*] Luca Dell'Amico,[2] Marcella Bonchio,[2] and Maurizio Prato[1,3,4,*]

SUMMARY

Carbon nanodots stand as the missing link between the molecular and the nanoscale world, owing to the unique molecular-like behavior emerging from their synthetic precursors. A converging set of analytical and spectroscopic data yields a precise inventory of the surface reactive groups of amine-rich carbon dots (NCDs-1). As a result, NCDs-1 provide a multi-functional nano-platform that is able to covalently activate carbonyl groups, form iminium-ions and enamine intermediates, and efficiently promote diverse amino-catalytic transformations in water. Remarkably, the catalytic activity of carbon dots can also govern the stereoselectivity in the bond-forming event. Indeed, the use of chiral carbon dots (NCDs-7) as catalysts affords the final aldol products with significant enantiomeric excess. The successful implementation of carbon nanostructures into chemical roles so far restricted to molecular systems opens new avenues for advanced applications where the nanoscale and the molecular realms will merge and complement each other.

INTRODUCTION

Carbon dots (CDs) are ultra-small, quasi-spherical, and non-toxic nanoparticles with a size below 10 nm, which typically show fluorescence properties and high solubility in aqueous and polar solvents.[1–17] CDs can be designed from readily available molecular precursors through straightforward and robust procedures so that their structural diversity and composition can be easily tailored for specific applications.[2–17] For these reasons, CDs are receiving increasing attention for biomedical applications, sensing, and opto-electronics.[18,19] Focusing on applications, the external shell composition, and the role of the terminal functional groups are of paramount importance. Indeed, the surface properties regulate their interaction with the surrounding environment in terms of recognition and binding, reactivity, solvation, as well as the material processability. Therefore, detailed characterization on the nature, amount, and accessibility of the surface terminal groups will bridge the gap between the nanoscale and the molecular scale, providing fundamental information to engineering the properties of these nanosized materials. This approach opens new synthetic opportunities via tailored CD synthesis or post-functionalization protocols and enables advanced applications such as catalytic transformations.[20–24] In particular, the appeal of CDs as nano-catalysts relate to their straightforward synthesis, cost-efficiency, and safety that, combined with high solubility in water, may allow their use even in biological or quasi-biological environments.[25–29] Despite their high potential, only exploratory applications of CDs as

The Bigger Picture

What is the breakthrough expected for the next-generation nanomaterial? The programming of its structure and functions using "green" synthetic and up-scaling protocols? Low toxicity and application in advanced technology platforms? In this vision, carbon nanodots are a potential game-changer among all other forms of nanomaterials. Carbon nanodots are obtained under hydrothermal conditions from a blend of molecular reagents whose properties turn out to be encoded within the final material. Herein, we show that amine-rich carbon nanodots display a prominent molecular behavior in terms of (1) acid-base properties, (2) distribution of amino domains with different chemical environments, probed by ^{19}F-tagging NMR spectroscopy, (3) formation of enamine and iminium catalytic intermediates, and (4) asymmetric catalysis. Carbon nanodots can, therefore, bridge the gap between homogeneous and heterogeneous catalysis, by transferring key molecular prerogatives at the horizon of nanoscale materials.

catalysts have been reported relying on simple acid-base or hydrogen-bonding activation modes.[20–23] Aminocatalysis represents one of the most versatile strategies in covalent organocatalytic transformations. The robustness of its activation modes, via enamine or iminium-ion intermediates, has been implemented in several synthetic applications addressing the requirements of step economy and metal-free catalysis. In addition, diverse aminocatalytic systems have been recently redesigned to allow catalytic activity in water media.[25] In light of these considerations, detailed information regarding the amount, diversity, and accessibility of surface functional groups would be extremely useful to implement CDs as covalent nanosized catalysts, a synthetic strategy largely unexplored.

An appealing trait of the bottom-up CD synthesis is that part of the functionalities of the starting molecular reagents are retained in the nanoparticle structure. Therefore, aiming at amine-rich CDs, for our study, we selected four frequently used CDs that are obtained from bottom-up synthesis involving readily available amines or their precursors (Figure 1).

Of particular interest are nitrogen-doped carbon nanodots obtained from the microwave-assisted hydrothermal reaction of arginine and ethylenediamine (NCDs-**1**).[12,30,31] The appeal of NCDs-**1** originates from the presence of 1,350 μmol/g of primary aliphatic amines, as measured by a standard Kaiser test (KT).[12,30,31] Moreover, other N-doped CDs were prepared from hydro or solvothermal protocols that employ citric acid in combination with urea (NCDs-**2**) or ethylenediamine (NCDs-**3**) as doping agents, as well as from the prolonged thermolysis of aspartic acid (100 h at 320°C, NCDs-**4**).[32–34] Furthermore, two other types of non-doped CDs, obtained from citric acid, were prepared for comparison: graphitic CDs-**5**, obtained in similar conditions as NCDs-**4**, and amorphous CDs-**6**, obtained upon a shorter thermolytic treatment at a lower temperature (40 h at 180°C) of the same precursor.[34,35]

Herein, we report how the detailed study and characterization of the terminal functional groups present in the CDs outer shell enables the identification of NCDs-**1** as unprecedented nano-platforms for covalent catalysis. Converging evidence obtained through multiple analytical and spectroscopic techniques, including AFM, DLS, electrophoretic studies, KT, pH titration, thermogravimetric analysis, IR spectroscopy, and *in situ* ^{19}F-NMR analysis, provides an accurate description of the surface amino groups present on NCDs-**1** at unprecedented levels of detail. This information gained to address the type, amount, accessibility, and reactivity of amine terminal groups unlocked the implementation of NCDs-**1** as efficient nano-catalysts in water media according to what are two fundamental aminocatalytic activation modes: the conjugate additions to α β-unsaturated aldehydes via electrophilic iminium-ion intermediates and the aldol reaction of ketones under nucleophilic enamine catalysis. Remarkably, the chiral derivative, i.e., the amine-rich (*S*)-NCDs-**7** is able to impart asymmetric induction in the bond-forming aldol event, demonstrating that the chiral information retained in the nanomaterial outer shell can be successfully transferred with molecular control, enabling the most desirable goal of enantioselective catalysis by carbon-based nanomaterials.

RESULTS AND DISCUSSION

Preliminary Studies

As the first step of our investigation, we evaluated the total number of acid/base sites present in the selected CDs. This was done using the Gran Plot analysis of simple pH back titrations, i.e., a linearization of the pH data affording

[1]CENMAT, Center of Excellence for Nanostructured Materials, Department of Chemical and Pharmaceutical Sciences, INSTM UdR Trieste, University of Trieste, Via Licio Giorgieri 1, Trieste 34127, Italy

[2]Department of Chemical Sciences University of Padova, Via Marzolo 1, Padova 35131, Italy

[3]Center for Cooperative Research in Biomaterials (CIC biomaGUNE), Basque Research and Technology Alliance (BRTA), Paseo de Miramón 182, 20014 Donostia-San Sebastián, Spain

[4]Ikerbasque, Basque Foundation for Science, Bilbao 48013, Spain

[5]Lead Contact

*Correspondence: gfilippini@units.it (G.F.), gragazzon@units.it (G.R.), xavier.companyo@unipd.it (X.C.), prato@units.it (M.P.)

https://doi.org/10.1016/j.chempr.2020.08.009

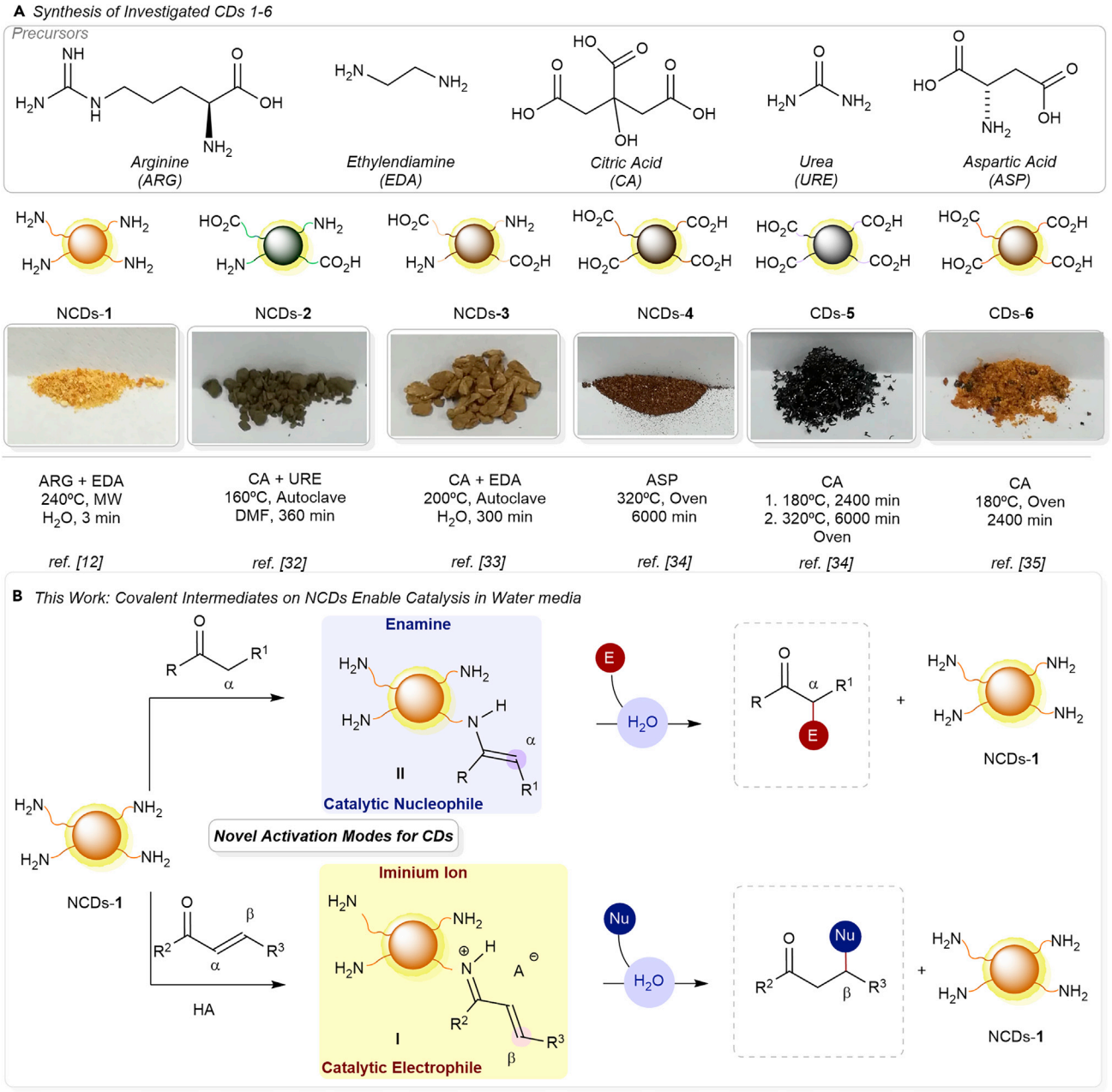

Figure 1. Overview of Investigated Carbon Dots and Target Application

(A) Precursors and synthesis of the investigated CDs.

(B) Aim of the work: application of NCDs-**1** in iminium-ion and enamine-mediated aminocatalytic processes in water media. MW, microwave; E, electrophile; Nu, nucleophile; HA, acidic additive.

the start- and end-point of the back titration, allowing the intended quantification.[36] Interestingly, despite the diversity of precursors and synthetic conditions, CDs displayed a number of acid/base sites in the order of 9,000 μmol/g in the interval from pH 12 to 3. CDs-**5** had the smallest number of acid/base sites. Indeed, the value of 11,000 μmol/g in CDs-**6** decreases to ca. 6,000 in CDs-**5**, as a result of a prolonged thermolysis, likely associated with decarboxylation reactions. A comparison of these values with those associated with the starting materials allows the quantification of the acid/base sites retained during the synthesis (Figure 2A).

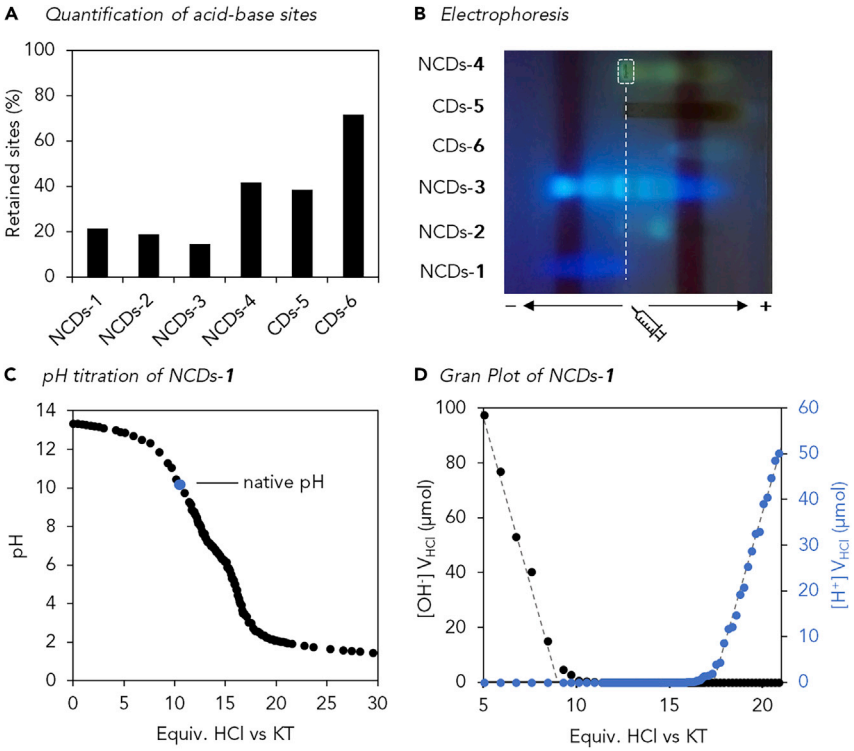

Figure 2. Screening of Carbon Dots

(A) Percentage of acid/base sites retained during the synthesis of each CDs.

(B) Postelectrophoresis photograph was taken under UV light (365 nm) of the gel at pH 7 containing all the investigated CDs.

(C) pH curve was observed upon back titration of NCDs-**1** (4.5 mg/mL) with HCl, after the addition of 10.5 equiv of NaOH versus the KT value at 120°C.

(D) Gran plot obtained from the data of Figure 2A; in the plateau region, the acid/base sites of NCDs-**1** are being protonated. See Figures S1–S14; Table S1 for details.

This analysis reveals more general trends: the extensive thermolysis affording CDs-**5** and NCDs-**4** induces a decrease in the number of retained sites, in both cases close to 40%. Moreover, in all the investigated multi-component synthesis only ca. 20% of the acid/base sites are retained, possibly as a consequence of amide-bond formation, that is reasonably occurring under hydrothermal conditions eventually following urea decomposition.[37]

To gain additional information on the surface charge and diversity of CDs, agarose gel electrophoresis was performed at neutral pH in phosphate buffer (Figure 2B; Supplemental Information). All CDs afforded broad bands. CDs-**6**, CDs-**5**, NCDs-**4**, and NCDs-**2** moved uniformly toward the anode, suggesting the presence of residual carboxylate functionalities. NCDs-**3** generated multiple bands that migrate toward both poles, in accordance with previous reports.[38] Differently from all other investigated CDs, NCDs-**1** migrated uniformly toward the cathode, indicating their positive charge at neutral pH, which could be consistent with the presence of protonated amino groups.

To complete the screening, the KT was performed on the various N-doped CDs. As expected, NCDs-**4** afforded a negative test, since the X-ray photoelectron spectroscopy data indicate the presence of nitrogen solely as pyrrolic or pyridinic.[34] Analysis of NCDs-**2** and NCDs-**3** revealed 1,000 and 1,100 µmol/g of primary aliphatic

amines, respectively, both values being lower than the reference value of 1,350 μmol/g associated to NCDs-**1**.[12,30]

Taken together, the data obtained from our preliminary studies point at NCDs-**1** as promising amine-rich platforms. While NCDs-**1** display a similar number of acid/base sites compared with other dots, they show a net positive charge—as evidenced by electrophoretic studies—and display the highest KT among all the studied CDs. For these reasons, we decided to focus our attention on NCDs-**1**.

The ultra-small size of NCDs-**1**, was confirmed by AFM analysis (see Figure S1), which confirmed a size of about 2.5 ± 0.8 nm.[12,30] The largely amorphous nature of NCDs-**1** was confirmed by thermogravimetric analysis (see Figure S1). Indeed, 94% of weight loss was observed at 600°C under nitrogen. Focusing on the molecular features of NCDs-**1**, infrared spectroscopy (see Figure S1) clearly points at the presence of N–H and O–H bonds involved in hydrogen-bond interactions, which provide solubility in water and polar solvents. An intense band at 1,654 cm^{-1} is compatible with the presence of amide bonds, which likely have a relevant role in the formation of NCDs-**1**. A solution of 4.5 mg/mL of NCDs-**1** in MilliQ water possesses a pH of 9.4, confirming the presence of basic sites in the sample. As-dissolved NCDs-**1** were completely deprotonated upon the addition of 10.5 equiv of NaOH with respect to the KT value (1,350 μmol/g). The back titration with HCl afforded the pH curve shown in Figure 2C. To our surprise, the minimum slope of the curve, which occurs in correspondence to the highest buffering capacity of NCDs-**1**, was obtained between pH 6 and 8, indicating the presence of several functional groups with a pK_a in that range. The observed pK_a value cannot be explained by the presence of simple primary aliphatic amines that typically have pK_a values around 11. However, such a low pK_a could be tentatively ascribed to the spatial proximity of non-protonated amines with other protonated groups, as observed in ethylenediamine, whose second protonation pK_a is 6.9.[39] Alternatively, the formation of imidazole derivatives, originating from the cyclization of ethylenediamine with guanidinium groups followed by aromatization, could provide an explanation.[40] Sites with pK_a close to physiological pH are employed by Nature as proton shuttles in a biological environment, thus NCDs-**1** may offer a multi-site environment for proton transfer under physiological conditions.[41]

The comparison between the total number of acid/base sites with the KT value in NCDs-**1** indicates that the number of acid/base (10,700 ± 800 μmol/g) sites is about 8 times higher with respect to the KT value (1,350 μmol/g, Figure 2D). Therefore, several acid/base sites present on the CD surface cannot be detected with the routinely performed KT. In fact, this colorimetric test exploits the condensation of primary aliphatic amines with ninhydrin forming an imine intermediate, thus requiring at least one hydrogen atom attached to the α-carbon of the reactive amine.[42,43] Secondary and aromatic amines are elusive under KT analysis while remaining of prominent interest as catalytic sites in organocatalytic schemes.

^{19}F-NMR Analysis

In order to obtain additional information on the main amine structural types, we studied the surface groups of NCDs-**1** by NMR spectroscopy. In this case, ^{1}H-NMR is not a suitable technique because the proton resonances of the NCDs-**1** span within a broad spectral region. Instead, we implemented a covalent fluorine-labeling strategy combined with ^{19}F-NMR analysis.[44] *p*-fluorocinnamaldehyde **1a** was selected as molecular fluorinated probe for two main reasons: (1) the well-established ability of cinnamaldehyde derivatives to condense with a large variety of primary and

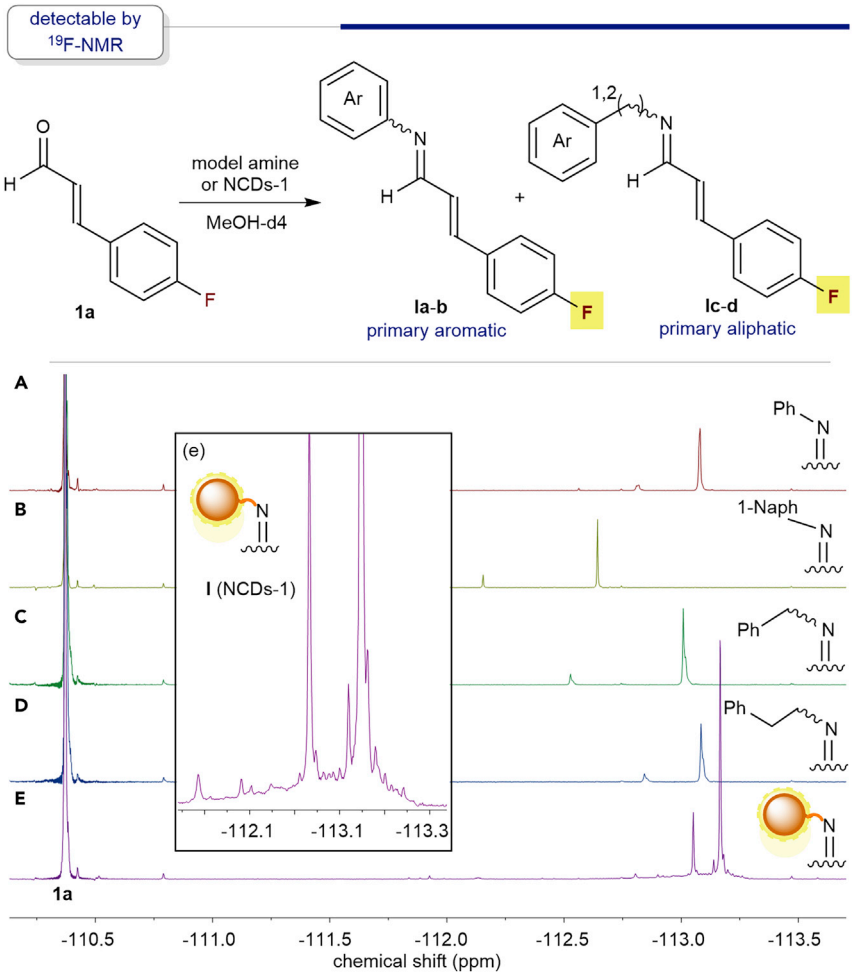

Figure 3. *In Situ* Imines Formation

(A–D) $^{19}F\{^{1}H\}$-NMR spectra of diverse imines **Ia–d** formed *in situ* upon the condensation of *p*-F-cinnamaldehyde **1a** (10 equiv, 0.125 mmol) with the corresponding model amines **2a–d** (1 equiv, 0.0125 mmol) in MeOH-d_4 after 24 h.

(E) ^{19}F-NMR spectra of NCDs-**1** solution (18 mg/mL) with **1a** (0.125 mmol) in MeOH-d_4 after 24 h.

secondary amines; (2) its condensation will give rise to conjugated imine or iminium-ion species, the actual electrophilic catalytic intermediates involved in aminocatalyzed conjugated additions.[45–49] In fact, the *in situ* condensation with the surface amines of NCDs-**1** would form the corresponding fluorinated imine or iminium-ion species, enabling the direct detection of the different fluorinated intermediates as a fingerprint of the surface functional groups. To validate this method, we chose a selection of model primary and secondary amines that are potentially representative of the population of the NCDs-**1** terminals, namely: aniline **2a** and 1-naphtylamine **2b** as aromatic primary amines, benzylamine **2c** and phenylethylamine **2d** as aliphatic primary amines, and dibenzylamine **2e** and diphenylamine **2f** as secondary amines. The mixture of *p*-fluorocinnamaldehyde **1a** with the aromatic (**2a–b**) and benzylic or aliphatic (**2c–d**) model primary amines afforded the corresponding fluorinated imines, unambiguously characterized by *in situ* ^{1}H and ^{19}F-NMR analyses (Figures 3A–3D and S13–S46).[50] Notably, the treatment of a NCDs-**1** solution (18 mg/mL) with 10 equiv of **1a** in MeOH-*d*4 showed, after 24 h, a set of broad ^{19}F-NMR resonances between −112.6 and −113.6 ppm that are ascribable to the

formation of fluorinated imines by covalent interaction between the tagged probe and the reactive groups on the NCDs-**1** surface (Figure 3E).

The use of *p*-fluorothioanisole as an internal standard allows a rough quantification of the surface imines that correspond to 4,100 μmol/g of available primary amines at the NCDs-**1** surface. Remarkably, this number is 3-fold higher compared with the KT value at 120°C (1,350 μmol/g), revealing that ^{19}F-NMR analysis with a fluorinated probe is a more effective technique for the determination of the available superficial primary amines. To expand the portfolio of detectable functional groups to secondary amines, we next implemented the fluorinated probe to the *in situ* generation of iminium-ion species (Figure 4).[51] Hence, the treatment of the different primary (**2a–d**) and secondary (**2e–f**) model amines with **1a** under acidic conditions afforded the corresponding fluorinated iminium ions **IIa–f** (Figures 4A–4G).[50] Interestingly, the ^{19}F{^{1}H}-NMR signals of the iminium ions formed in solution are more sensitive to structural variations with respect to the imines.

The ^{19}F{^{1}H}-NMR analysis of the solution NCDs-**1** (18 mg/mL) with 4 equiv of **1a** and 4 equiv of trichloroacetic acid (TCA) in MeOH-*d*4 is shown in Figure 4G, which clearly shows the appearance of a new set of signals corresponding to the iminium ions generated between the fluorinated aldehyde **1a** with the surface amine groups. By comparison with the model iminium-ions spectra (Figures 4A–4F), we were able to identify three main amine types present in the NCDs-**1** external surface as: (1) secondary aliphatic amines, (2) primary aromatic amines, and (3) primary aliphatic amines. Instead, as shown in Figure 4, secondary aromatic amines, such as diphenyl amine **2f**, are not present on NCDs-**1** surface. In agreement with the imine ^{19}F{^{1}H}-NMR (Figure 3) and with the titration experiments (Figure 2), the major type of reactive groups present on the NCDs-**1** surface turn out to be aliphatic primary amines.

The ^{19}F{^{1}H}-NMR quantification on the imines revealed a 3-fold enhancement in the determination of the amount of available reactive amine with respect to classical KT analysis and accounts approximately for the 40% of all the acid/base active sites predicted by the titration experiments. With these studies, we have established ^{19}F{^{1}H}-NMR as a useful and fast technique for the determination of the amine content on the NCDs-**1** surface.

Kaiser Test Studies

To gain more information on the accessibility of the terminal amines, we performed a deeper investigation of the KT on NCDs-**1** using benzylamine (**2c**) as the model amine. As expected, under the standard conditions (120°C for 15 min) both NCDs-**1** and benzylamine afforded a positive test, with a quantitative conversion of the latter. Additionally, the normalized absorption spectra for the two samples were almost identical (Figure 5A), confirming that the KT can be safely performed on NCDs-**1** unlike some simple amines such as proline or ethylenediamine (see Supplemental Information). To test the hypothesis of a limited accessibility of amines at room temperature, additional KTs were performed at room temperature and followed in time (Figure 5B). Under these conditions, the conversion of benzylamine remained quantitative (see Supplemental Information). On the other hand, taking the results of the KT at 120°C as a reference, the conversion of NCDs-**1** leveled off at around 64% ± 7%. These experiments confirmed the hypothesis of a limited accessibility of the amines at room temperature. Taking this factor into consideration, the actual amount of primary amino groups within NCDs-**1** might be even higher than the value measured through ^{19}F-NMR analysis at ambient temperature (4,100 μmol/g). Thus, assuming a similar accessibility for all amino moieties (about

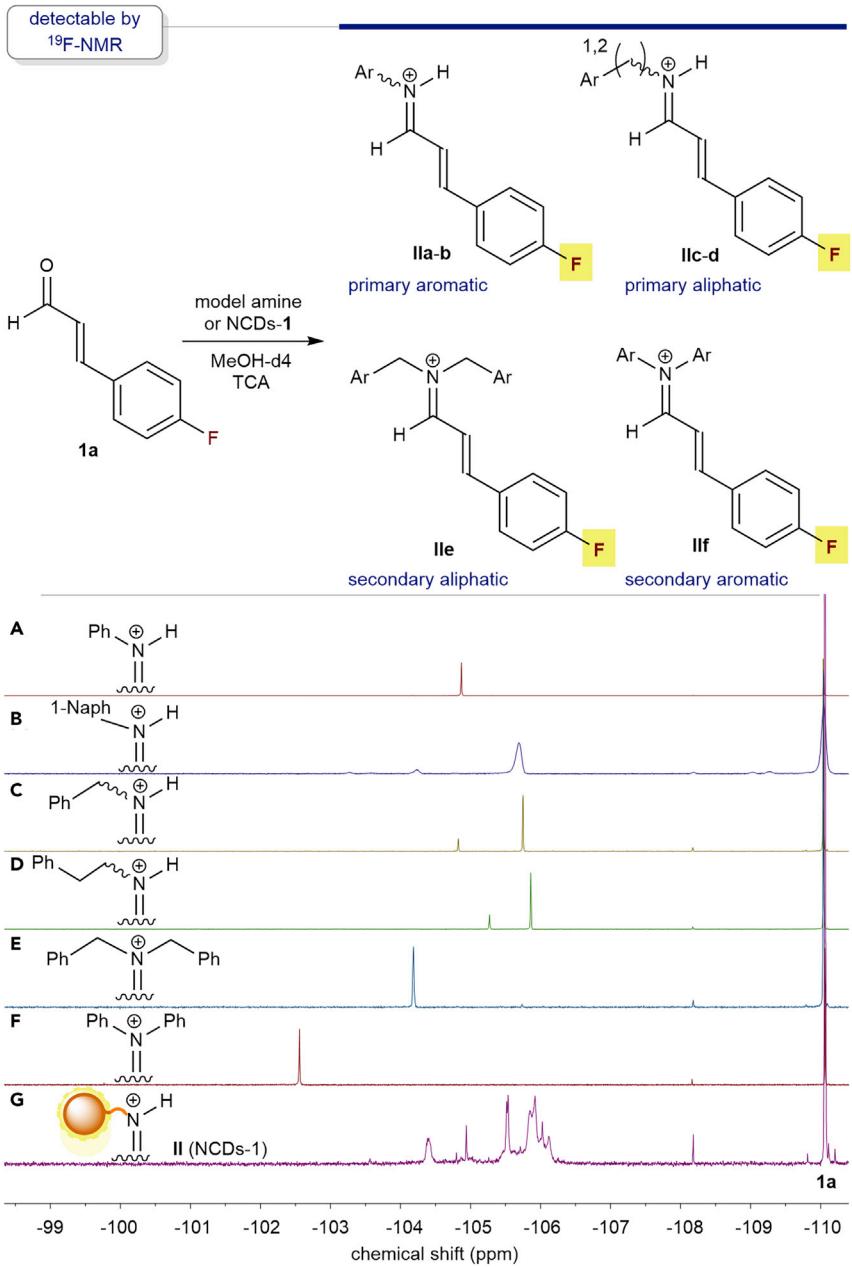

Figure 4. *In Situ* Iminium-Ion Formation

(A–F) $^{19}F\{^{1}H\}$-NMR traces of the diverse iminium ions **IIa–f** formed upon condensation of *p*-F-cinnamaldehyde **1a** (4 equiv, 0.4 mmol) and trichloroacetic acid (TCA) (4 equiv, 0.4 mmol) with the corresponding model amines **2a–f** (1 equiv, 0.1 mmol).

(G) $^{19}F\{^{1}H\}$-NMR spectra of NCDs-1 solution (18 mg/mL) with **1a** (0.4 mmol) and TCA (1 mmol) in MeOH-d_4.

64%), a calculated overall value of approximately 6,400 μmol/g of primary amines for NCDs-1 could be tentatively proposed.

This rationalization suggests that a high portion of the acid/base active sites on the surface of NCDs-1 are primary amines, albeit some are less accessible to carbonyl compounds and, therefore, not reactive at room temperature. These deductions

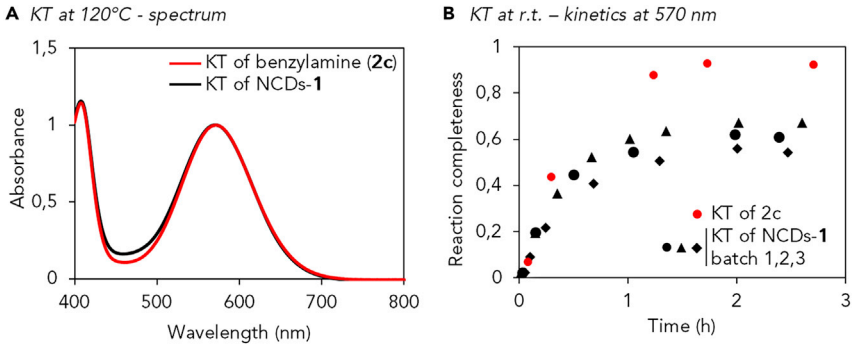

Figure 5. Kaiser Test Studies

(A) Normalized absorption spectra recorded, performing the KT at 120°C of benzylamine (**2c**, red) and NCDs-**1** (black).

(B) Representative kinetic traces observed at 570 nm while monitoring the KT at room temperature of **2c** (red dots) and three batches of NCDs-**1** (black indicators).

are also consistent with the positive charge observed with electrophoresis as well as with the elemental analysis of NCDs-**1** (*C* 62%, *H* 9%, *N* 21%, and *O* 7%). These data would assign to *N* 9% of the total weight of NCDs-**1**, and the residual 12% *N* content could be reasonably present in undetected moieties, such as amides, that are known to form at relatively low temperature during CD synthesis, and heterocycles or secondary amines, that cannot be quantified via imine formation.[52] The experiments presented so far establish both the nature and the amount of available primary amines located on the surface of the NCDs-**1**. Such a detailed characterization becomes of fundamental importance for the implementation of CDs in advanced applications relying on the chemical behavior of their surface.

N-Doped Carbon Nanodots as Aminocatalysts

Building on the extensive characterization of the amino-rich CDs domains, we envisioned the use of NCDs-**1** as water-soluble catalysts tackling the activation of aldehydes and ketones, which are both expected to occur vis-à-vis the structural diversity of the reactive amine groups identified by ^{19}F-NMR.[53–59] Indeed, the iminium-ion species detected by *in situ* NMR analysis are the electrophilic catalytic intermediates responsible for the LUMO-lowering activation in aminocatalysis, able to engage in conjugate addition with a series of nucleophiles.[60–62] To this aim, we first evaluated the reactivity between *p*-F-cinnamaldehyde (**1a**) and *N*-methylindole (**3a**) as biologically relevant *C*-nucleophile.[63] Operating in methanol, the conditions at which the iminium ions (II) were identified on the surface of NCDs-**1** (Figure 4G), a catalytic amount of NCDs-**1** (3.6% w/v), and trifluoroacetic acid (TFA) (20 mol %) furnished the product **4a** in 47% yield (Figure 6). An optimization study revealed that in the water-dioxane 1:1 mixture, the reaction occurs smoothly, delivering the product **4a** in 63% isolated yield (Figure 6) similarly to well-established aminocatalytic systems.[60–62] The catalytic activity of NCDs-**1** was then compared with that of free-model amines— i.e., **2a**, **2d**, **2e**, and pyrrolidine— demonstrating that in all cases, NCDs-**1** outperforms the isolated amine precursors in terms of the substrate conversion and product yield (see Table S4 and Figure S63). To prove the generality of NCDs-**1** as a water-compatible catalytic system for iminium-ion activation, different carbonyl compounds (**1a–d**) and nucleophiles (**2a** or **3a–e**) were tested, affording the corresponding β-funtionalized products **4a–h** in isolated yields spanning from 53% to 92% (see Figures S64–S72). Control experiments confirmed the envisaged aminocatalytic scheme by NCDs-**1**. In the absence of NCDs-**1**, the conjugate addition of dimethyl malonate (**3b**) to cyclohexenone (**1c**) is completely suppressed (Figure 6, **4c**, 0% yield). Also, the catalytic performance is strongly inhibited in the absence of

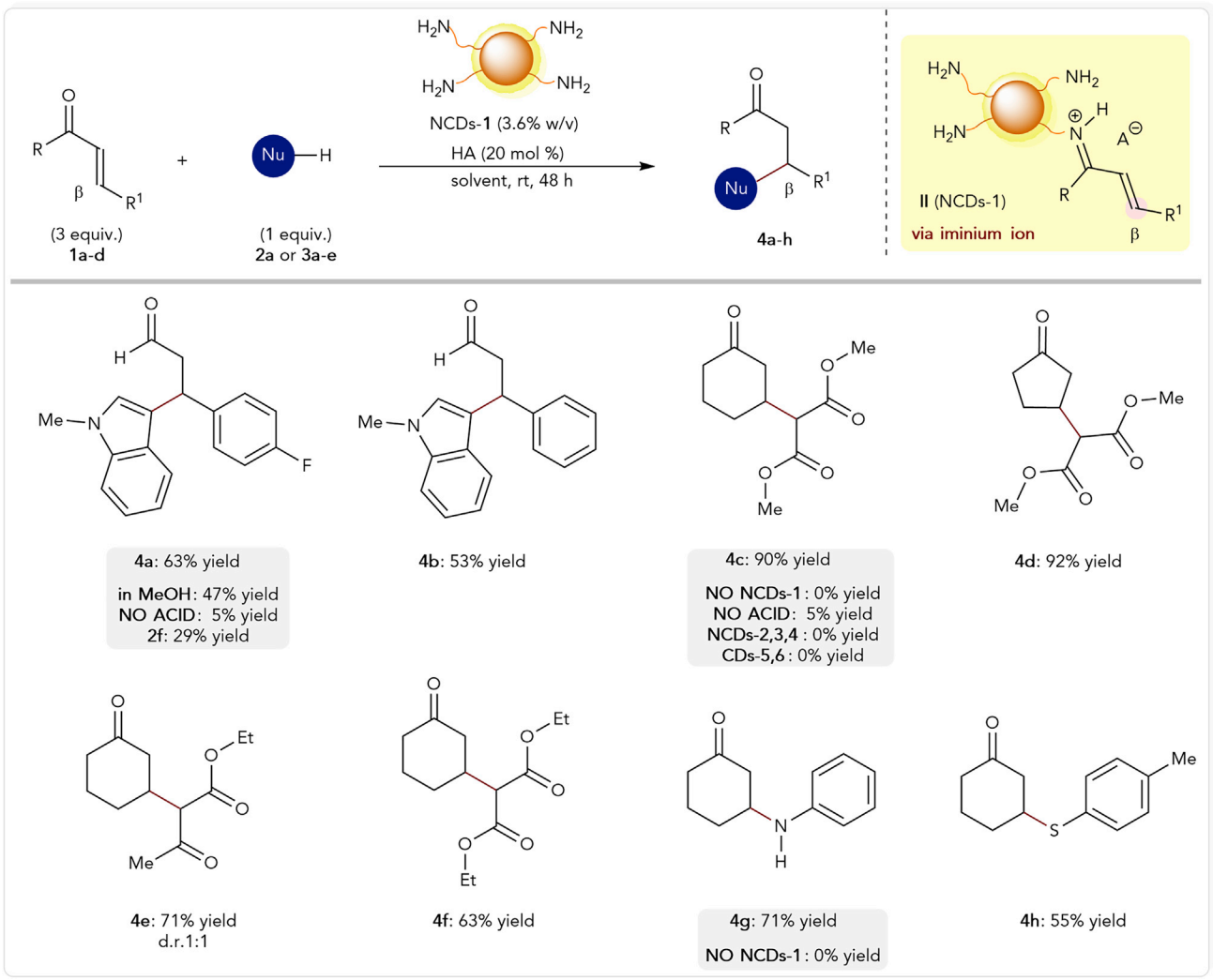

Figure 6. Aminocatalysis via Iminium Ion

NCDs-**1**-catalyzed conjugate additions of different nucleophiles (**2a** or **3a–e**) to enals and enones **1a–d**. Reaction was performed on 0.1 mmol scale. TFA and dioxane/MilliQ water (1:1) were used for the synthesis of compounds **4a–b**. Benzoic acid (HA) and pure MilliQ water were used for the synthesis of compounds **4c–h**. Yields of the isolated products are indicated below each entry.

acid (Figure 6, **4c**, 5% yield), delineating a close correlation with the ^{19}F-NMR experiments in which the presence of acid was essential for the formation of the iminium-ions intermediates **II** (Figure 4).

The requirement of surface amines that are able to condense with the carbonyl compounds was further corroborated by the use of CDs where nitrogen sites are present solely as pyridinic and pyrrolic-type residues (NCDs-**4**) or nitrogen-free CDs (CDs-**5** and CDs-**6**).[34] In both cases, the product **4c** was not formed. Further, NCDs-**2** and NCDs-**3**, which afforded a positive KT, were also tested as catalysts, however, displaying a broad structural inhomogeneity, as evidenced by their multiple-band electrophoretic behavior (Figure 2B). Even in these cases, the product **4c** was not detected, thus indicating that a stringent control of CD surface environment and composition is crucial for reactivity.

To expand the portfolio of catalytic activation modes performed by the NCDs-**1**, we turned our attention to the formation of enamine intermediates toward

HOMO-rising catalysis.[53–59,64] In fact, primary and secondary amines can also be used to catalyze the enamine-mediated addition of α-enolizable aldehydes and ketones to electrophiles. After the screening of the diverse reaction parameters, we found that the present nanosized catalytic platform successfully activates simple acetone (**1e**) toward aldol-type addition to isatin derivatives (**5**) in pure MilliQ water. We then studied the generality and limitations of the proposed aldol protocol catalyzed by NCDs-**1** (0.9% w/v). A diverse set of isatins was transformed into the corresponding 3,3-disubstituted oxindole derivatives (Figures 7A and S73–S81). Thus, isatins **5a–e** bearing both electron-withdrawing and electron-donating substituents afforded the corresponding products **6a–e** in excellent isolated yields (81%–96%). Moreover, 2-pentanone **1f** and the cyclic ketones cyclohexanone **1g** and cycloheptanone **1h** actively participated in the catalytic functionalization of isatin (products **6f–h**). Remarkably, products **6g–h** were obtained with complete diastereocontrol (d.r. > 20:1). The observed selectivity likely originates in the increased steric hindrance of cyclic ketones **1g** and **1h**. Furthermore, common water sources, such as tap water and seawater, can also be used as solvents, providing **6a** in comparable excellent yields. This demonstrates the robustness of the described methodology to variations of pH and ionic strength in the reaction medium.

Building on these results, we applied the NCDs-**1**-catalyzed protocol to the synthesis of Convolutamydine A (**6i**) in 60% isolated yield (Figure 7B). It is worth mentioning that (*R*)-Convolutamydine A is a natural product with a potent inhibitory activity on the differentiation of HL-60 human promyelocytic leukemia cells and can be successfully synthesized as a racemic mixture using NCDs-**1** as a catalyst in water.[65–67]

Finally, we turned our attention toward the challenging implementation of asymmetric catalysis by chiral CD derivatives.[68] So far, the use of carbon nanomaterials in enantioselective transformations has only been addressed relying on post-functionalization procedures.[69,70] While, due to the harsh synthetic reaction conditions, the enantiopure building blocks undergo racemization generally leading to optically inactive CDs, as in the case of NCDs-**1**,[17] recently, chiral NCDs (NCDs-**7**) have been successfully prepared by employing (*R*,*R*)- or (*S*,*S*)-1,2-cyclohexanediamine in combination with L-arginine as precursors (Figure 8A).[17] Therefore, we studied the catalytic behavior of (*S*)-NCDs-**7** in the aldol addition of acetone **1e** to isatin **5a** under enamine catalysis conditions (Figure 8B; Table S2). The reaction in aqueous media at room temperature affords the aldol adduct (*S*)-**6a** quantitatively (99% yield) with 6% of enantiomeric excess (ee). Importantly, the direct use of (*S*,*S*)-1,2-cyclohexanediamine as catalyst under the same reaction conditions yields the final product in 62% yield and with ee as low as 4%. The poorer performance of (*S*,*S*)-1,2-cyclohexanediamine confirms again the superior catalytic activity of the NCDs in comparison with the free-amine constituents, demonstrating that the inclusion of chiral diamines into the carbon-based nanomaterial scaffold enhances their catalytic activity while preserving a similar asymmetric induction. By lowering the reaction temperature to 0°C the enantiocontrol imparted by the chiral nanosized catalytic platform can be increased to 9%. Interestingly, when dichloromethane is used as a solvent, the final aldol adduct (*S*)-**6a** is formed with a remarkable and reproducible 38% ee (see Figures S15 and S16). To the best of our knowledge, these results represent the first example of asymmetric catalysis promoted by a chiral CD nanomaterial, whereby molecular chirality is transferred at the nanoscale. Notably, the isolated (*S*,*S*)-1,2-cyclohexanediamine probed under analogous experimental conditions provides a similar enhancement of asymmetric induction (46% ee), albeit with a much lower product yield (25%). These results highlight the still unexplored

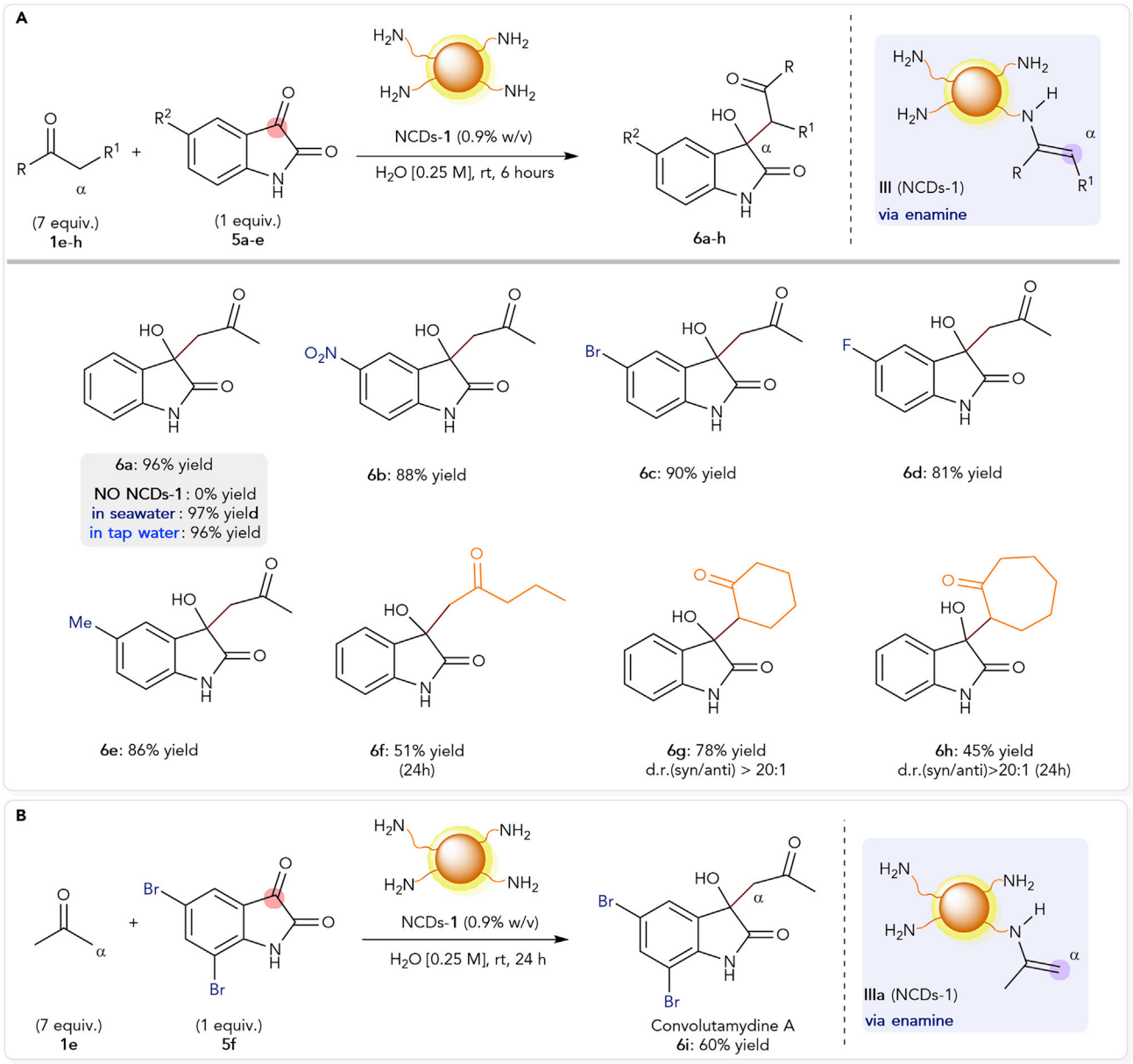

Figure 7. Aminocatalysis via Enamine and Synthesis of Biologically Active Convolutamydine A

(A) NCDs-**1**-catalyzed aldol additions of ketones **1e–h** to isatins **5a–e**. Reactions were performed on 0.1 mmol scale using MilliQ water. Yields and diastereoselectivities of the isolated products are indicated below each entry. For the synthesis of compounds **6f** and **6h**, the reactions were performed over 24 h.

(B) NCDs-**1**-catalyzed aldol additions of acetone (**1e**) to 5,7-dibromoisatin (**5f**). The reaction was performed on 0.1 mmol scale using MilliQ water.

potential of carbon nanomaterials for enantioselective recognition and do confirm the effective molecular encoding of CDs for asymmetric catalysis.

Conclusion

The use of a wide set of analytical and spectroscopic molecular techniques provides unprecedented evidence on the nature, amount, availability, and reactivity of terminal amino functionalities present in the outer shell of commonly used CDs. This knowledge reveals that nitrogen-rich CDs exhibit a unique molecular-like behavior

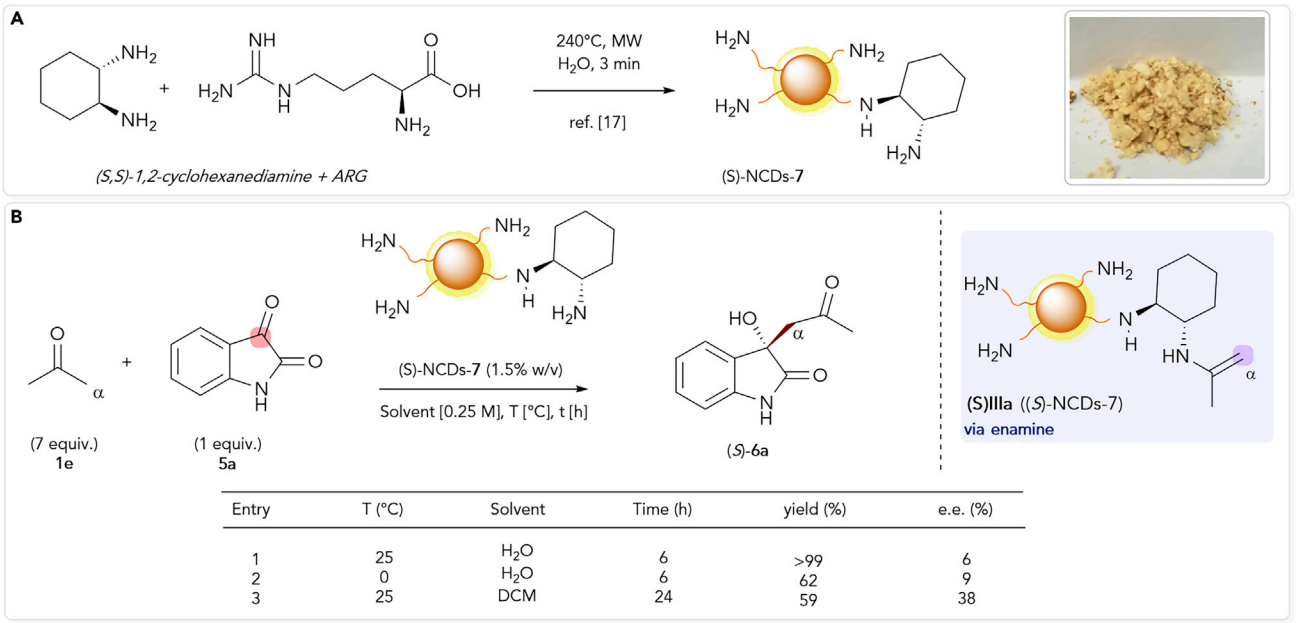

Figure 8. Enantioselective Catalysis Using Chiral CDs

(A) Synthesis of chiral (*S*)-NCDs-**7**.

(B) (*S*)-NCDs-**7** catalyzed aldol addition of acetone (**1e**) to isatin (**5a**). Reactions were performed on 0.1 mmol scale.

while retaining the typical nanocolloidal features. As a result, these nanosized multifunctional materials have been successfully implemented into amino-catalyzed reactivity schemes enabling the activation of carbonyl compounds via covalent bonding in water solution. Different benchmark aminocatalytic transformations, including conjugate additions and aldol reactions, are efficiently catalyzed by NCDs catalysts proceeding via iminium-ion and enamine intermediates. Furthermore, the use of optically active CDs as catalysts allows to govern the stereodetermining bond-forming event, demonstrating that the chirality retained in the CD outer shell can be transferred with molecular control in the catalytic process. In summary, this study proves that the accurate characterization of the nanomaterial surface enables advanced applications commonly considered out of reach for nanostructures, such as covalent asymmetric catalysis, and provides the proof of principle for the implementation of nanomaterials into chemical roles previously considered only attainable by the molecular realm.

EXPERIMENTAL PROCEDURES

Resource Availability

Lead Contact

Further information and requests for resources and reagents should be directed to and will be fulfilled by the Lead Contact, Giulio Ragazzon (gragazzon@units.it).

Materials Availability

This study did not generate new unique reagents.

Data and Code Availability

This study did not generate datasets or codes.

Full experimental procedures are provided in the Supplemental Information.

SUPPLEMENTAL INFORMATION

Supplemental Information can be found online at https://doi.org/10.1016/j.chempr.2020.08.009.

ACKNOWLEDGMENTS

M.P. is the AXA Chair for Carbon Bionanotechnology (2016-2023). This work was supported by the Universities of Trieste and Padova, INSTM, the Italian Ministry of Education MIUR (cofin Prot. 2017PBXPN4), the Spanish Ministry of Science, Innovation and Universities, MICIU (project PID2019-108523RB-I00), the CariPARO Foundation SYNERGY (L.D.), as well as by the GREEN C-C STARS starting grant (X.C.). C.R. thanks the European Social Fund, Operational Programme 2014/2020 Friuli-Venezia Giulia (regional code FP1799043001) for a doctoral fellowship. A.V.-P. thanks the Seal of Excellence @unipd PLACARD for a postdoctoral fellowship. This work was performed under the Maria de Maeztu Units of Excellence Program from the Spanish State Research Agency grant no. MDM-2017-0720. The authors thank Prof. Andrea Sartorel for helpful discussions and Dr. Francesco Rigodanza for the DLS analyses.

AUTHOR CONTRIBUTIONS

M.P. and M.B. obtained funding; F.A. and G.R. performed carbon dots screening; A.V., X.C., and L.D. performed NMR studies; G.F. and C.R. performed organocatalytic studies. M.P., G.R., A.V., X.C., L.D., and M.B. validated the data. G.F., G.R., and X.C. wrote the manuscript with contributions from all authors.

DECLARATION OF INTERESTS

The authors declare no competing interests.

Received: March 21, 2020
Revised: May 29, 2020
Accepted: August 13, 2020
Published: September 10, 2020

REFERENCES

1. Baker, S.N., and Baker, G.A. (2010). Luminescent carbon nanodots: emergent nanolights. Angew. Chem. Int. Ed. Engl. *49*, 6726–6744.

2. Georgakilas, V., Perman, J.A., Tucek, J., and Zboril, R. (2015). Broad family of carbon nanoallotropes: classification, chemistry, and applications of fullerenes, carbon dots, nanotubes, graphene, nanodiamonds, and combined superstructures. Chem. Rev. *115*, 4744–4822.

3. Lim, S.Y., Shen, W., and Gao, Z. (2015). Carbon quantum dots and their applications. Chem. Soc. Rev. *44*, 362–381.

4. Roy, P., Chen, P.-C., Periasamy, A.P., Chen, Y.-N., and Chang, H.-T. (2015). Photoluminescent carbon nanodots: synthesis, physicochemical properties and analytical applications. Mater. Today *18*, 447–458.

5. Sun, Y.-P., Zhou, B., Lin, Y., Wang, W., Fernando, K.A.S., Pathak, P., Meziani, M.J., Harruff, B.A., Wang, X., Wang, H., et al. (2006). Quantum-sized carbon dots for bright and colorful photoluminescence. J. Am. Chem. Soc. *128*, 7756–7757.

6. Arcudi, F., Đorđević, L., and Prato, M. (2017). Rationally designed carbon nanodots towards pure white-light emission. Angew. Chem. Int. Ed. Engl. *56*, 4170–4173.

7. Hutton, G.A.M., Martindale, B.C.M., and Reisner, E. (2017). Carbon dots as photosensitisers for solar-driven catalysis. Chem. Soc. Rev. *46*, 6111–6123.

8. Li, H., Kang, Z., Liu, Y., and Lee, S.-T. (2012). Carbon nanodots: synthesis, properties and applications. J. Mater. Chem. *22*, 24230–24253.

9. Rigodanza, F., Đorđević, L., Arcudi, F., and Prato, M. (2018). Customizing the electrochemical properties of carbon nanodots by using quinones in bottom-up synthesis. Angew. Chem. Int. Ed. Engl. *57*, 5062–5067.

10. Cringoli, M.C., Kralj, S., Kurbasic, M., Urban, M., and Marchesan, S. (2017). Luminescent supramolecular hydrogels from a tripeptide and nitrogen-doped carbon nanodots. Beilstein J. Nanotechnol. *8*, 1553–1562.

11. Gomez, I.J., Arnaiz, B., Cacioppo, M., Arcudi, F., and Prato, M. (2018). Nitrogen-doped carbon nanodots for bioimaging and delivery of paclitaxel. J. Mater. Chem. B *6*, 5540–5548.

12. Arcudi, F., Đorđević, L., and Prato, M. (2016). Synthesis, separation, and characterization of small and highly fluorescent nitrogen-doped carbon nanodots. Angew. Chem. Int. Ed. Engl. *55*, 2107–2112.

13. Carrara, S., Arcudi, F., Prato, M., and De Cola, L. (2017). Amine-rich nitrogen-doped carbon nanodots as a platform for self-enhancing electrochemiluminescence. Angew. Chem. Int. Ed. Engl. *56*, 4757–4761.

14. Arcudi, F., Strauss, V., Đorđević, L., Cadranel, A., Guldi, D.M., and Prato, M. (2017). Porphyrin antennas on carbon nanodots: excited state energy and electron transduction. Angew. Chem. Int. Ed. Engl. *56*, 12097–12101.

15. Hill, S.A., Benito-Alifonso, D., Morgan, D.J., Davis, S.A., Berry, M., and Galan, M.C. (2016).

Three-minute synthesis of sp^3 nanocrystalline carbon dots as non-toxic fluorescent platforms for intracellular delivery. Nanoscale *8*, 18630–18634.

16. Mazzier, D., Favaro, M., Agnoli, S., Silvestrini, S., Granozzi, G., Maggini, M., and Moretto, A. (2014). Synthesis of luminescent 3D microstructures formed by carbon quantum dots and their self-assembly properties. Chem. Commun. (Camb.) *50*, 6592–6595.

17. Đorđević, L., Arcudi, F., D'Urso, A., Cacioppo, M., Micali, N., Bürgi, T., Purrello, R., and Prato, M. (2018). Design principles of chiral carbon nanodots help convey chirality from molecular to nanoscale level. Nat. Commun. *9*, 3442.

18. Molaei, M.J. (2019). Carbon quantum dots and their biomedical and therapeutic applications: a review. RSC Adv. *9*, 6460–6481.

19. Li, X., Rui, M., Song, J., Shen, Z., and Zeng, H. (2015). Carbon and graphene quantum dots for optoelectronic and energy devices: a review. Adv. Funct. Mater. *25*, 4929–4947.

20. Testa, C., Zammataro, A., Pappalardo, A., and Trusso Sfrazzetto, G. (2019). Catalysis with carbon nanoparticles. RSC Adv. *9*, 27659–27664.

21. Han, Y., Huang, H., Zhang, H., Liu, Y., Han, X., Liu, R., Li, H., and Kang, Z. (2014). Carbon quantum dots with photoenhanced hydrogen-bond catalytic activity in aldol condensations. ACS Catal. *4*, 781–787.

22. Majumdar, B., Mandani, S., Bhattacharya, T., Sarma, D., and Sarma, T.K. (2017). Probing Carbocatalytic activity of carbon nanodots for the synthesis of biologically active dihydro/Spiro/glyco quinazolinones and Aza-Michael adducts. J. Org. Chem. *82*, 2097–2106.

23. Pei, X., Xiong, D., Wang, H., Gao, S., Zhang, X., Zhang, S., and Wang, J. (2018). Reversible phase transfer of carbon dots between an organic phase and aqueous solution triggered by CO_2. Angew. Chem. Int. Ed. Engl. *57*, 3687–3691.

24. Rosso, C., Filippini, G., and Prato, M. (2019). Use of nitrogen-doped carbon nanodots for the photocatalytic fluoroalkylation of organic compounds. Chemistry *25*, 16032–16036.

25. van der Helm, M.P., Klemm, B., and Eelkema, R. (2019). Organocatalysis in aqueous media. Nat. Rev. Chem. *3*, 491–508.

26. Lindström, U.M. (2002). Stereoselective organic reactions in water. Chem. Rev. *102*, 2751–2772.

27. Chanda, A., and Fokin, V.V. (2009). Organic synthesis "on water". Chem. Rev. *109*, 725–748.

28. Simon, M.O., and Li, C.J. (2012). Green chemistry oriented organic synthesis in water. Chem. Soc. Rev. *41*, 1415–1427.

29. Jimeno, C. (2016). Water in asymmetric organocatalytic systems: a global perspective. Org. Biomol. Chem. *14*, 6147–6164.

30. Đorđević, L., Arcudi, F., and Prato, M. (2019). Preparation, functionalization and characterization of engineered carbon nanodots. Nat. Protoc. *14*, 2931–2953.

31. Arcudi, F., Đorđević, L., and Prato, M. (2019). Design, synthesis, and functionalization strategies of tailored carbon nanodots. Acc. Chem. Res. *52*, 2070–2079.

32. Li, D., Jing, P., Sun, L., An, Y., Shan, X., Lu, X., Zhou, D., Han, D., Shen, D., Zhai, Y., et al. (2018). Near-infrared excitation/emission and multiphoton-induced fluorescence of carbon dots. Adv. Mater. *30*, e1705913.

33. Schneider, J., Reckmeier, C.J., Xiong, Y., von Seckendorff, M., Susha, A.S., Kasák, P., and Rogach, A.L. (2017). Molecular fluorescence in citric acid-based carbon dots. J. Phys. Chem. C *121*, 2014–2022.

34. Martindale, B.C.M., Hutton, G.A.M., Caputo, C.A., Prantl, S., Godin, R., Durrant, J.R., and Reisner, E. (2017). Enhancing light absorption and charge transfer efficiency in carbon dots through graphitization and core nitrogen doping. Angew. Chem. Int. Ed. Engl. *56*, 6459–6463.

35. Martindale, B.C.M., Hutton, G.A.M., Caputo, C.A., and Reisner, E. (2015). Solar hydrogen production using carbon quantum dots and a molecular nickel catalyst. J. Am. Chem. Soc. *137*, 6018–6025.

36. Boiani, J.A. (1986). The Gran plot analysis of an acid mixture: an undergraduate experiment to highlight this alternate method. J. Chem. Educ. *63*, 724–726.

37. Schaber, P.M., Colson, J., Higgins, S., Thielen, D., Anspach, B., and Brauer, J. (2004). Thermal decomposition (pyrolysis) of urea in an open reaction vessel. Thermochim. Acta *424*, 131–142.

38. Ehrat, F., Bhattacharyya, S., Schneider, J., Löf, A., Wyrwich, R., Rogach, A.L., Stolarczyk, J.K., Urban, A.S., and Feldmann, J. (2017). Tracking the source of carbon dot photoluminescence: aromatic domains versus molecular fluorophores. Nano Lett. *17*, 7710–7716.

39. Nan, Z., and Tan, Z.-C. (2005). Thermodynamic Investigation of the Azeotropic Binary Mixture water + *n*-propanol. J. Chem. Eng. Data *50*, 6–10.

40. Bucio-Cano, A., Reyes-Arellano, A., Correa-Basurto, J., Bello, M., Torres-Jaramillo, J., Salgado-Zamora, H., Curiel-Quesada, E., Peralta-Cruz, J., and Avila-Sorrosa, A. (2015). Targeting quorum sensing by designing azoline derivatives to inhibit the N-hexanoyl homoserine lactone-receptor CviR: synthesis as well as biological and theoretical evaluations. Bioorg. Med. Chem. *23*, 7565–7577.

41. Schneider, F. (1978). Histidine in enzyme active centers. Angew. Chem. Int. Ed. Engl. *17*, 583–592.

42. Troll, W., and Cannan, R.K. (1953). A modified photometric Ninhydrin method for the analysis of amino and imino acids. J. Biol. Chem. *200*, 803–811.

43. Sarin, V.K., Kent, S.B.H., Tam, J.P., and Merrifield, R.B. (1981). Quantitative monitoring of solid-phase peptide synthesis by the Ninhydrin reaction. Anal. Biochem. *117*, 147–157.

44. Sun, Y., Kunc, F., Balhara, V., Coleman, B., Kodra, O., Raza, M., Chen, M., Brinkmann, A., Lopinski, G.P., and Johnston, L.J. (2019). Quantification of amine functional groups on silica nanoparticles: a multi-method approach. Nanoscale Adv. *1*, 1598–1607.

45. Brazier, J.B., Jones, K.M., Platts, J.A., and Tomkinson, N.C.O. (2011). On the roles of protic solvents in imidazolidinone-catalyzed transformations. Angew. Chem. Int. Ed. Engl. *50*, 1613–1616.

46. Gotoh, H., Uchimaru, T., and Hayashi, Y. (2015). Two reaction mechanisms via iminium ion intermediates: the different reactivities of diphenylprolinol silyl ether and trifluoromethyl-substituted diarylprolinol silyl ether. Chemistry *21*, 12337–12346.

47. Günler, Z.I., Companyó, X., Alfonso, I., Burés, J., Jimeno, C., and Pericàs, M.A. (2016). Deciphering the roles of multiple additives in organocatalyzed Michael additions. Chem. Commun. (Camb.) *52*, 6821–6824.

48. Companyó, X., and Burés, J. (2017). Distribution of catalytic species as an indicator to overcome reproducibility problems. J. Am. Chem. Soc. *139*, 8432–8435.

49. Renzi, P., Hioe, J., and Gschwind, R.M. (2017). Enamine/dienamine and brønsted acid catalysis: elusive intermediates, reaction mechanisms, and stereoinduction modes based on in situ NMR spectroscopy and computational studies. Acc. Chem. Res. *50*, 2936–2948.

50. The minor peak present in the 19F NMR traces of the imine Ia–Id and iminium ions IIb–IId correspond to the less stable cis-isomers. See Supplemental Information Section F, Figures S17– S62 for further information.

51. During the NMR analysis of the aromatic amines (aniline 2a and 1-naphtylamine 2b) performed in the presence of p-F-cinnamladehyde 1a and TCA, we observed a rapid decomposition of the corresponding iminium ion species. This process hampered the possibility to performing accurate quantification experiments involving the generation of iminium ion intermediates with the NCDs-1.

52. Vallan, L., Urriolabeitia, E.P., Ruipérez, F., Matxain, J.M., Canton-Vitoria, R., Tagmatarchis, N., Benito, A.M., and Maser, W.K. (2018). Supramolecular-enhanced charge transfer within entangled polyamide chains as the origin of the universal blue fluorescence of polymer carbon dots. J. Am. Chem. Soc. *140*, 12862–12869.

53. Lelais, G., and MacMillan, D.W.C. (2006). Modern strategies in organic catalysis: the advent and development of iminium activation. Aldrichimica Acta *39*, 79–87.

54. Melchiorre, P., Marigo, M., Carlone, A., and Bartoli, G. (2008). Asymmetric aminocatalysis—gold rush in organic chemistry. Angew. Chem. Int. Ed. Engl. *47*, 6138–6171.

55. Bertelsen, S., and Jørgensen, K.A. (2009). Organocatalysis—after the gold rush. Chem. Soc. Rev. *38*, 2178–2189.

56. Melchiorre, P. (2012). Cinchona-based primary amine catalysis in the asymmetric functionalization of carbonyl compounds. Angew. Chem. Int. Ed. Engl. *51*, 9748–9770.

57. Donslund, B.S., Johansen, T.K., Poulsen, P.H., Halskov, K.S., and Jørgensen, K.A. (2015). The

Diarylprolinol silyl ethers: ten years after. Angew. Chem. Int. Ed. Engl. *54*, 13860–13874.

58. Reyes-Rodríguez, G.J., Rezayee, N.M., Vidal-Albalat, A., and Jørgensen, K.A. (2019). Prevalence of Diarylprolinol silyl ethers as catalysts in total synthesis and patents. Chem. Rev. *119*, 4221–4260.

59. Vega-Peñaloza, A., Paria, S., Bonchio, M., Dell'Amico, L., and Companyó, X. (2019). Profiling the privileges of pyrrolidine-based catalysts in asymmetric synthesis: From polar to light-driven radical chemistry. ACS Catal. *9*, 6058–6072.

60. Erkkilä, A., Majander, I., and Pihko, P.M. (2007). Iminium catalysis. Chem. Rev. *107*, 5416–5470.

61. Seebach, D., Gilmour, R., Grošelj, U., Deniau, G., Sparr, C., Ebert, M.-O., Beck, A.K., McCusker, L.B., Šišak, D., and Uchimaru, T. (2010). Stereochemical models for discussing additions to α,β-unsaturated aldehydes organocatalyzed by diarylprolinol or imidazolidinone derivatives – is there an '(E)/(Z)-dilemma'? Helv. Chim. Acta *93*, 603–634.

62. Rios, R., and Companyó, X. (2013). Addition to α,β-unsaturated aldehydes and ketones. In Comprehensive Enantioselective Organocatalysis, P.I. Dalko, ed. (Wiley-VCH), pp. 977–1008.

63. Austin, J.F., and MacMillan, D.W.C. (2002). Enantioselective organocatalytic indole alkylations. Design of a new and highly effective chiral amine for iminium catalysis. J. Am. Chem. Soc. *124*, 1172–1173.

64. Mukherjee, S., Yang, J.W., Hoffmann, S., and List, B. (2007). Asymmetric enamine catalysis. Chem. Rev. *107*, 5471–5569.

65. Kamano, Y., Zhang, H.-P., Ichihara, Y., Kizu, H., Komiyama, K., and Pettit, G.R. (1995). Convolutamydine A, a novel bioactive hydroxyoxindole alkaloid from marine bryozoan *Amathia convoluta*. Tetrahedron Lett. *36*, 2783–2784.

66. Zhang, H.-P., Kamano, Y., Ichihara, Y., Kizu, H., Komiyama, K., Itokawa, H., and Pettit, G.R. (1995). Isolation and structure of convolutamydines B∼ D from marine bryozoan *Amathia convolute*. Tetrahedron *51*, 5523–5528.

67. Nakamura, S., Hara, N., Nakashima, H., Kubo, K., Shibata, N., and Toru, T. (2008). Enantioselective synthesis of (R)-convolutamydine A with new N-heteroarylsulfonylprolinamides. Chemistry *14*, 8079–8081.

68. Rosso, C., Filippini, G., and Prato, M. (2020). Carbon dots as nano-organocatalysts for synthetic applications. ACS Catal. *10*, 8090–8105.

69. Chronopoulos, D.D., Kokotos, C.G., Tsakos, M., Karousis, N., Kokotos, G., and Tagmatarchis, N. (2015). Conjugating proline derivatives onto multi-walled carbon nanotubes: preparation, characterization and catalytic activity in water. Mater. Lett. *157*, 212–214.

70. Rosso, C., Emma, M.G., Martinelli, A., Lombardo, M., Quintavalla, A., Trombini, C., Syrgiannis, Z., and Prato, M. (2019). A recyclable chiral 2-(triphenylmethyl) pyrrolidine organocatalyst anchored to [60] fullerene. Adv. Synth. Catal. *361*, 2936–2944.